Interfacing formate dehydrogenase with metal oxides for reversible electrocatalysis and solar-driven reduction of carbon dioxide

Melanie Miller,[a] William E. Robinson,[a] Ana Rita Oliveira,[b] Nina Heidary,[a] Nikolay Kornienko,[a] Julien Warnan,[a] Inês A. C. Pereira,[b] Erwin Reisner*[a]

Abstract: *The integration of enzymes with synthetic materials allows efficient electrocatalysis and solar fuels production. Here, we couple formate dehydrogenase (**FDH**) from Desulfovibrio vulgaris Hildenborough (DvH) to metal oxides for catalytic CO_2 reduction and report an in-depth study of the resulting enzyme-material interface. Protein film voltammetry (PFV) demonstrates stable binding of **FDH** on metal oxide electrodes and reveals reversible and selective reduction of CO_2 to formate. Quartz crystal microbalance (QCM) and attenuated total reflection infrared (ATR-IR) spectroscopy confirm a high binding affinity for **FDH** to the TiO_2 surface. Adsorption of **FDH** on dye-sensitized TiO_2 allows for visible-light driven CO_2 reduction to formate in the absence of a soluble redox mediator with a turnover frequency (TOF) of 11 ± 1 s^{-1}. The strong coupling of the enzyme to the semiconductor gives rise to a new benchmark in selective photoreduction of aqueous CO_2 to formate.*

Electrocatalytic and solar-driven fuel synthesis from the greenhouse gas CO_2 is a desirable approach to simultaneously produce sustainable energy carriers and combat increasing atmospheric CO_2 levels.[1] Formate is a stable intermediate in the reduction of CO_2 and can be used as liquid energy carrier in fuel cells, as hydrogen storage material, or feedstock for the synthesis of fine chemicals.[2] Metals and synthetic molecular systems are widely studied as electrocatalysts for CO_2 reduction to formate, but largely lack the required efficiency, selectivity or affordability to enable carbon capture and utilization technologies.[3,4]

There is avid research in both biological and artificial CO_2 fixation. Semi-artificial photosynthesis provides a common stage for these contrasting approaches as components from synthetic and biological origin can be combined in hybrid model systems.[5] To date, enzyme-based visible-light driven CO_2 reduction to formate relies on diffusional mediators such as methyl viologen (MV^{2+}) and nicotinamide adenine dinucleotide (NAD^+).[6,7] Mediated processes are inefficient as they consume energy, are kinetically slow and cause short-circuit reactions. MV^{2+} is toxic to microorganisms,[8] and NAD^+ is prohibitively expensive for fuel production.[6]

[a] M. Miller, Dr. W. E. Robinson, Dr. N. Heidary, Dr. N. Kornienko, Dr. J. Warnan, Prof. E. Reisner
Department of Chemistry, University of Cambridge
Cambridge CB2 1EW (United Kingdom)
E-mail: reisner@ch.cam.ac.uk
Web: http://www-reisner.ch.cam.ac.uk/

[b] A. R. Oliveira, Prof. I. A. C. Pereira
Instituto de Tecnologia Química e Biológica António Xavier
Universidade Nova de Lisboa
Av. da República, 2780-157 Oeiras (Portugal)

Supporting information for this article is given *via* a link at the end.

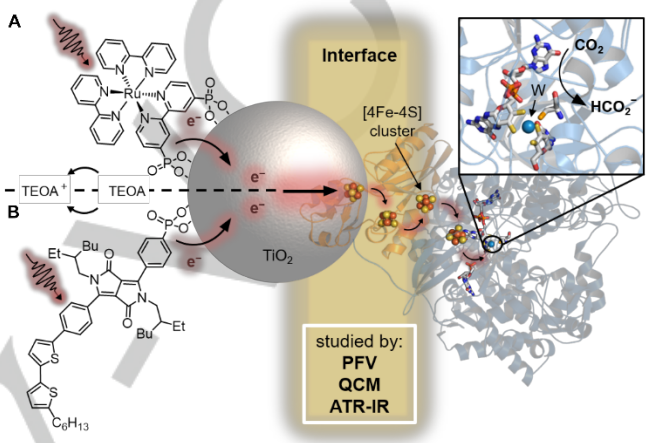

Figure 1. Schematic CO_2 conversion with a semiconductor-**FDH** photocatalyst system. Photoexcited electrons from the dye, **RuP** in (A) or **DPP** in (B), are transferred via the conduction band (CB) of TiO_2 across the enzyme-material interface through the intraprotein [4Fe-4S] relays to the W-active site of **FDH** for the reduction of CO_2 to formate. The oxidized dye is regenerated by triethanolamine (TEOA). A protein structure homologous to *Dv*H **FDH** is shown.[9]

In this work, we have selected **FDH** from *Dv*H as it has previously displayed robustness and high activity for the reduction of CO_2 and oxidation of formate in solution assays.[10,11] Initially, PFV was employed to study interfacial electron transfer between **FDH** and porous indium-doped tin oxide (ITO) and TiO_2 electrodes in the absence of a mediator. Immobilization and loading of **FDH** on TiO_2 were then investigated using a QCM and ATR-IR spectroscopy. **FDH** was finally coupled directly to dye-sensitized TiO_2 nanoparticles to enable photocatalytic reduction of CO_2 selectively to formate in a diffusional mediator-free colloidal system (Figure 1).

The electrocatalytic activity of **FDH** on metal oxide electrodes was studied by PFV on mesoporous ITO (*meso*ITO) and TiO_2 (*meso*TiO_2) electrodes with a film thickness of approximately 2.5 µm (Figure S1).[12,13] **FDH** (21.5 µM) was activated by incubation with the reducing agent *DL*-dithiotreitol (DTT, 50 mM)[9] and the resulting solution (2 µL) was drop cast on the electrode surface. The **FDH**-modified electrode was placed in an electrolyte solution containing CO_2/$NaHCO_3$ and KCl at pH 6.5 under a CO_2 atmosphere.

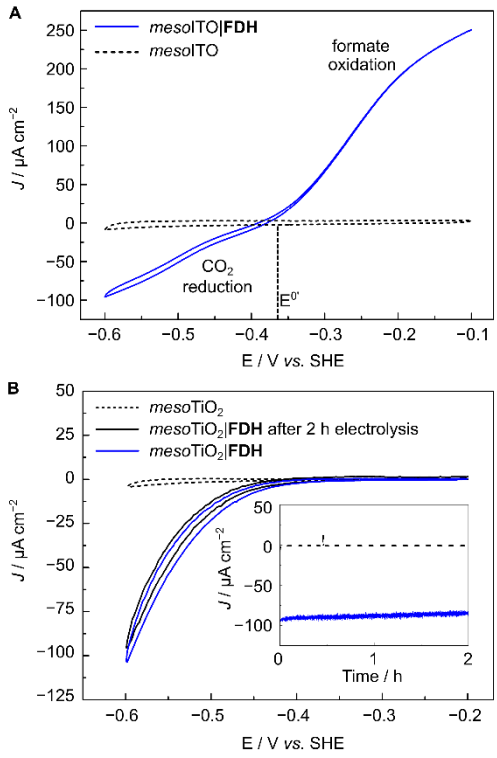

Figure 2. PFV (ν = 5 mV s^{-1}) showing (A) reversible reduction of CO_2 to formate by *meso*ITO|**FDH** (blue trace) and (B) CO_2 reduction by *meso*TiO_2|**FDH** before (blue) and after 2 h CPE (black). Inset: CPE at −0.6 V *vs.* SHE. Conditions: 43 pmol **FDH** (amount drop-cast), 100 mM CO_2/$NaHCO_3$, 50 mM KCl, 20 mM formate (only present in A), 1 atm CO_2, pH 6.5, 25°C, Pt counter electrode. Dashed traces show control experiments of **FDH**-free electrodes.

Figure 2A shows the electrochemically reversible interconversion of CO_2 and formate by **FDH** immobilized on a conductive *meso*ITO electrode (*meso*ITO|**FDH**). The onset potential for both CO_2 reduction and formate oxidation was observed close to the thermodynamic potential ($E^{0'}$ = −0.36 V *vs.* SHE, pH 6.5),[14] demonstrating that interfacial electron transfer by the [4Fe-4S] relays and catalysis at the W-active site are highly efficient.[15] Similar electrochemically reversible characteristics have been previously reported for **FDH**s from *Escherichia coli* and *Syntrophobacter fumaroxidans* on graphite electrodes,[14,16,17] but not for *Dv*H **FDH** or for any **FDH** on metal oxide electrodes.

When **FDH** was immobilized on a semiconducting *meso*TiO_2 electrode (*meso*TiO_2|**FDH**), a similar onset potential for CO_2 reduction (−0.4 V *vs.* SHE) was observed and the current density reached −100 µA cm^{-2} at −0.6 V *vs.* SHE (Figure 2B). Formate oxidation cannot be observed for *meso*TiO_2|**FDH** electrodes as TiO_2 behaves as an insulator at the required potentials. Controlled-potential electrolysis (CPE) at −0.6 V *vs.* SHE for 2 h produced formate with a Faradaic efficiency of (92 ± 5)% (Figure 2B, inset). Comparison of PFV scans before and after CPE showed that 92% of the initial **FDH** activity remains after 2 h, demonstrating the excellent stability of the immobilized enzyme.

The interaction of **FDH** and TiO_2 was quantitatively investigated with a previously described QCM cell.[18,19] Upon flowing an **FDH**-containing solution over a *planar*TiO_2-covered quartz chip (12 nM in 100 mM TEOA), the surface of TiO_2 reached saturation after 1 h, resulting in approximately 3.5 pmol cm^{-2} of adsorbed **FDH** (*planar*TiO_2|**FDH**; Figure 3A). The strength of the enzyme - TiO_2 interaction was probed by exposing the *planar*TiO_2|**FDH** electrode to buffer solutions with different ionic strengths. Rinsing the QCM cell with an enzyme-free solution for 1 h desorbed only 6% of the preloaded **FDH**. Changing to higher KCl concentrations showed that 70 - 60% of **FDH** remained adsorbed on the TiO_2 surface at 0.5 - 3.0 M KCl. Maintaining 60% loading of **FDH** on TiO_2 after multiple rinsing steps with high KCl concentrations suggests a contribution from chemisorption for the attachment of the enzyme.[20,21] Amino acid residues exposed on the FDH surface are likely involved in binding. For example, aspartic and glutamic acid have previously been shown to form a strong interaction with TiO_2.[22,23]

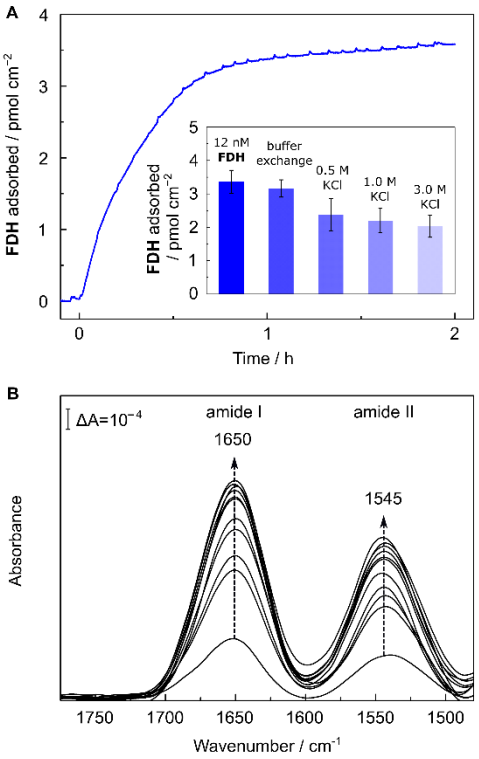

Figure 3: (A) QCM analysis of the adsorption process of **FDH** on a *planar*TiO_2-coated quartz chip. Conditions: 12 nM **FDH,** 100 mM TEOA, open circuit potential of −0.1 to 0.0 V *vs.* SHE, pH 6.5, 25°C, N_2 atmosphere, circulation (0.141 mL min^{-1}). Inset: Desorption of **FDH** by replacing the solution with fresh solution (100 mM TEOA) and subsequent increase of the ionic strength (each condition was held for 1 h). Error bars correspond to standard deviation (N = 3). (B) ATR-IR absorbance spectra of amide band region of **FDH** during the adsorption process over time onto *planar*TiO_2 coated Si prism (100 nm thickness). Arrows indicate successive spectra every 1.5 min up to 7.5 min and then every 30 min. Conditions: 1.0 µM **FDH,** 100 mM TEOA, total volume: 150 µl, open circuit potential, pH 6.5, 25°C.

Adsorption of **FDH** was also probed by surface-selective ATR-IR spectroscopy using a Si prism coated with a *planar* and a *meso*TiO_2 layer (100 and 400 nm thickness, respectively). After addition of **FDH** to the buffer solution covering the *planar*TiO_2 (Figure 3B) or *meso*TiO_2 (Figure S2) coated prism, the two

characteristic amide I and amide II bands of the protein backbone structure were detected at 1650 cm^{-1} and 1545 cm^{-1}.[24] The protein adsorption was monitored *in situ* over 2 h of incubation time and no (*planar*TiO_2) or slight (*meso*TiO_2) changes of the band features in the amide band region were observed, suggesting a mainly retained backbone structure of **FDH** on the surface of TiO_2. During the adsorption process, amide I and amide II band intensities showed an increase over time (Figure S3). The majority of **FDH** remained adsorbed on the surface of *planar*TiO_2 (Figure S3) upon increasing the ionic strength of the buffer, which agrees with the QCM experiments (Figure 3A, inset) and supports a stronger than purely electrostatic interaction between **FDH** and TiO_2.

After establishing the strong interface between **FDH** and TiO_2, visible-light-driven CO_2 reduction to formate was investigated with **FDH** immobilized on dye-sensitized TiO_2 nanoparticles (dye|TiO_2|**FDH**, Figures 1 and 4). The colloidal system was self-assembled by adding **FDH** pre-activated with DTT to a suspension of TiO_2 nanoparticles containing TEOA and a phosphonate group-bearing dye, either a ruthenium tris-2,2'-bipyridine complex (**RuP**) or a diketopyrrolopyrrole (**DPP**) at pH 6.5 and 25°C under N_2 atmosphere to protect the enzyme from aerobic damage. Both dyes are known to adsorb on TiO_2 via their phosphonate anchoring groups and **DPP** provides a precious-metal free alternative to **RuP**.[25] CO_2 was introduced to the solution via the addition of $NaHCO_3$. Upon UV-filtered irradiation, the photoexcited dye injects electrons into the CB of TiO_2 ($E_{CB}(TiO_2)$= −0.67 V *vs.* SHE at pH 6.5),[25] whereupon the electrons are conveyed to the catalytic W-center of **FDH** to drive CO_2 reduction. The oxidized dye is regenerated by the sacrificial electron donor (Figure 1).[26]

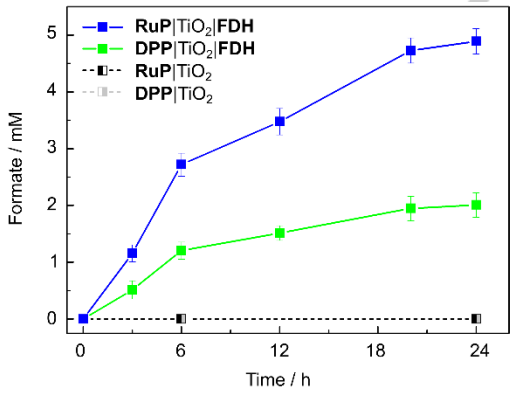

Figure 4. Photocatalytic CO_2 reduction to formate with **FDH** in a colloidal dye-sensitized TiO_2 system. Conditions: 12 nM **FDH**, 10 mM DTT, 0.83 mg mL^{-1} TiO_2, 16.7 µM dye (**RuP** or **DPP**), 100 mM TEOA, 100 mM $NaHCO_3$, pH 6.5, 25°C, total volume: 1.0 mL, assembled in an anaerobic glove box, UV-filtered simulated solar light irradiation: 100 mW cm^{-2}, AM 1.5G, λ > 420 nm. Error bars correspond to standard deviation (N = 3). Dashed traces show control experiments in the absence of **FDH**.

The dye|TiO_2|**FDH** systems show stable formate production for approximately 6 h (Figure 4). The formation of gaseous or dissolved side-products was not detected by ion chromatography, gas chromatography and ^{1}H NMR spectroscopy. The activity of **RuP**|TiO_2|**FDH** was not limited by the amount of dye or light intensity (Figures S4 and S5). A solution assay monitoring the activity of **FDH** by UV-vis spectroscopy (via formate oxidation in presence of 2 mM MV^{2+}) showed that approximately 36 ± 7% **FDH** remained active after 24 h photocatalysis (Figure S6), suggesting that denaturation of **FDH** is the main reason for activity loss. The addition of MV^{2+} as a soluble redox mediator to **RuP**|TiO_2|**FDH** showed that not all **FDH** present in the system is accessible by direct electron transfer across the enzyme-material interface (Figure S7). Control experiments demonstrated that all components are essential for formate production (Figures S8 and S9) and support oxidative quenching and 'through-particle' electron transfer as depicted in Figure 1 (Figure S10 and S11).[26] Isotopic labelling studies confirmed that formate was produced from CO_2 (Figure S12).

Table 1. Comparison of TOFs for dye-sensitized TiO_2 systems with enzymatic and synthetic catalysts for H_2 evolution and CO_2 reduction.

reaction	dye	catalyst	TOF / h^{-1}	ref.
$CO_2 \rightarrow HCO_2^-$	**RuP**	*DvH* **FDH**[a]	4.0×10^4	this work
	DPP	*DvH* **FDH**[a]	1.8×10^4	this work
$CO_2 \rightarrow CO$	**RuP**	*Ch* CODH I[b]	5.4×10^2	[27]
	dye[c]	**Re**[d]	8.6	[28]
$H^+ \rightarrow H_2$	**RuP**	*Db* [NiFeSe]-H_2ase[e]	1.8×10^5	[22]
	DPP	*Db* [NiFeSe]-H_2ase[e]	8.7×10^3	[25]
	CN_x[f]	*Db* [NiFeSe]-H_2ase[e]	2.8×10^4	[23]
	RuP	**NiP**[g]	3.2×10^2	[29]

[a] W-**FDH** from *Dv*H, [b] Carbon monoxide dehydrogenase (CODH) I from *Carboxydothermus hydrogenoformans* (*Ch*), [c] (E)-2-cyano-3-(5'-(5''-(p-(diphenylamino)phenyl)thiophen-2''-yl)thiophen-2'-yl)-acrylic acid, [d] synthetic rhenium catalyst in *N,N*-dimethyl formamide (DMF) and water, [e] [NiFeSe]-hydrogenase from *Desulfomicrobium baculatum (Db),* [f] polyheptazine carbon nitride polymer melon (CN_x), [g] nickel(II) bis(diphosphine) catalyst (**NiP**).

For photocatalytic experiments, an enzyme loading of approximately 0.03 pmol cm^{-2} was calculated assuming that all **FDH** is adsorbed on TiO_2 with a surface area of 50 m^2 g^{-1}. Saturation of the TiO_2 surface with **FDH** in the QCM experiment was only observed when two orders of magnitude higher amounts of **FDH** were adsorbed (Figure 3A). As QCM and ATR-IR spectroscopy indicate stronger than purely electrostatic interactions, close-to-quantitative adsorption of **FDH** on the TiO_2 nanoparticle in the colloidal system is likely. A TOF of 11 ± 1.0 and 5 ± 0.6 s^{-1} (based on CO_2 conversion after 6 h) and approximately 4.9 ± 0.2 and 2.0 ± 0.2 µmol formate (after 24 h)

were observed from CO_2 using **RuP** and **DPP**-sensitized TiO_2, respectively (Figure 4). The results of all photocatalysis experiments are presented in Tables S1 and S2.

Table 1 shows a comparison of state-of-the-art catalysts (enzymatic and synthetic) in combination with dye-sensitized TiO_2 nanoparticles without diffusional mediators for CO_2 reduction and H_2 evolution. Previous studies showed that enzymes clearly outperform the synthetic systems in terms of TOF.[30] Among the compared systems, the presented **RuP**|TiO_2|**FDH** system exhibits the highest TOF for CO_2 reduction. **DPP**|TiO_2|**FDH** shows that comparable activities can also be achieved in an entirely precious metal-free system. In semi-artificial systems, rapid electron transfer from TiO_2 to the enzyme was previously found to be essential for efficient catalysis,[22,31] suggesting that the strong interfacial interaction plays an important role for the high activity and stability of dye|TiO_2|**FDH**. Previously reported photocatalyst systems employing NAD^+ dependent FDHs for CO_2 reduction to formate rely on soluble redox mediators and only produced TOFs in the range of 10-20 h^{-1}.[32]

In summary, **FDH** immobilized on metal oxide electrodes is established as a reversible electrocatalyst for the selective conversion of CO_2 to formate. The porous metal oxide scaffolds allow for high **FDH** loading and consequently high current densities, which makes the protein-modified electrodes not only a relevant model system for CO_2 utilization, but also for formate oxidation in formate fuel cells. An excellent interface between TiO_2 and **FDH** is confirmed by QCM and ATR-IR spectroscopy. The direct (diffusional mediator-free) electron transfer across the enzyme-metal oxide interface is exploited for visible-light-driven CO_2 reduction to formate. Our results underline the importance of characterizing the interactions at the enzyme-material interface and future improvements in performance may arise from more controlled immobilization and more efficient electron transfer with the directly wired **FDH**.

Acknowledgements

This work was supported by an ERC Consolidator Grant "MatEnSAP" (682833), the Royal Society (NF160054, Newton fellowship), the Christian Doppler Research Association and OMV Group, SFRH/BD/116515/2016, grant PTDC/BIA-MIC/2723/2014 and R&D units UID/Multi/04551/2013 (Green-IT) and LISBOA-01-0145-FEDER-007660 (Most-Micro) cofunded by FCT/MCTES and FEDER funds through COMPETE2020/POCI and European Union's Horizon 2020 research and innovation programme (GA 810856). We thank Prof. J. Hirst, Dr. A. Eisenschmidt, Dr. S. Roy, A. Wagner and D. Antón García for fruitful discussions.

Keywords: artificial photosynthesis • carbon dioxide fixation • formate dehydrogenase • interfaces • photocatalysis

[1] D. G. Nocera, *Acc. Chem. Res.* **2017**, *50*, 616–619.
[2] A. Boddien, D. Mellmann, F. Gartner, R. Jackstell, H. Junge, P. J. Dyson, G. Laurenczy, R. Ludwig, M. Beller, *Science* **2011**, *333*, 1733–1736.
[3] S. Gao, Y. Lin, X. Jiao, Y. Sun, Q. Luo, W. Zhang, D. Li, J. Yang, Y. Xie, *Nature* **2016**, *529*, 68–71.
[4] K. E. Dalle, J. Warnan, J. J. Leung, B. Reuillard, I. S. Karmel, E. Reisner, *Chem. Rev.* **2019**, *in press*, DOI 10.1021/acs.chemrev.8b00392.
[5] N. Kornienko, J. Z. Zhang, K. K. Sakimoto, P. Yang, E. Reisner, *Nat. Nanotechnol.* **2018**, *13*, 890–899.
[6] J. Kim, S. H. Lee, F. Tieves, D. S. Choi, F. Hollmann, C. E. Paul, C. B. Park, *Angew. Chemie Int. Ed.* **2018**, *57*, 13825–13828.
[7] B. A. Parkinson, P. F. Weaver, *Nature* **1984**, *309*, 148–149.
[8] S. F. Rowe, G. Le Gall, E. V. Ainsworth, J. A. Davies, C. W. J. Lockwood, L. Shi, A. Elliston, I. N. Roberts, K. W. Waldron, D. J. Richardson, et al., *ACS Catal.* **2017**, *7*, 7558–7566.
[9] H. Raaijmakers, S. Macieira, J. M. Dias, S. Teixeira, S. Bursakov, R. Huber, J. J. G. Moura, I. Moura, M. J. Romão, *Structure* **2002**, *10*, 1261–1272.
[10] S. M. da Silva, C. Pimentel, F. M. A. Valente, C. Rodrigues-Pousada, I. A. C. Pereira, *J. Bacteriol.* **2011**, *193*, 2909–2916.
[11] S. M. da Silva, J. Voordouw, C. Leitao, M. Martins, G. Voordouw, I. A. C. Pereira, *Microbiology* **2013**, *159*, 1760–1769.
[12] T. E. Rosser, M. A. Gross, Y.-H. Lai, E. Reisner, *Chem. Sci.* **2016**, *7*, 4024–4035.
[13] M. Kato, T. Cardona, A. W. Rutherford, E. Reisner, *J. Am. Chem. Soc.* **2012**, *134*, 8332–8335.
[14] T. Reda, C. M. Plugge, N. J. Abram, J. Hirst, *Proc. Natl. Acad. Sci. U. S. A.* **2008**, *105*, 10654–10658.
[15] F. A. Armstrong, J. Hirst, *Proc. Natl. Acad. Sci. U. S. A.* **2011**, *108*, 14049–14054.
[16] A. Bassegoda, C. Madden, D. W. Wakerley, E. Reisner, J. Hirst, *J. Am. Chem. Soc.* **2014**, *136*, 15473–15476.
[17] W. E. Robinson, A. Bassegoda, E. Reisner, J. Hirst, *J. Am. Chem. Soc.* **2017**, *139*, 9927–9936.
[18] N. Kornienko, N. Heidary, G. Cibin, E. Reisner, *Chem. Sci.* **2018**, *9*, 5322–5333.
[19] D. H. Nam, J. Z. Zhang, V. Andrei, N. Kornienko, N. Heidary, A. Wagner, K. Nakanishi, K. P. Sokol, B. Slater, I. Zebger, et al., *Angew. Chemie Int. Ed.* **2018**, *57*, 10595–10599.
[20] S. Frasca, T. von Graberg, J. J. Feng, A. Thomas, B. M. Smarsly, I. M. Weidinger, F. W. Scheller, P. Hildebrandt, U. Wollenberger, *ChemCatChem* **2010**, *2*, 839–845.
[21] H. K. Ly, M. A. Marti, D. F. Martin, D. Alvarez-Paggi, W. Meister, A. Kranich, I. M. Weidinger, P. Hildebrandt, D. H. Murgida, *ChemPhysChem* **2010**, *11*, 1225–1235.
[22] E. Reisner, D. J. Powell, C. Cavazza, J. C. Fontecilla-Camps, F. A. Armstrong, *J. Am. Chem. Soc.* **2009**, *131*, 18457–18466.
[23] C. A. Caputo, L. Wang, R. Beranek, E. Reisner, *Chem. Sci.* **2015**, *6*, 5690–5694.
[24] A. Barth, *Biochim. Biophys. Acta - Bioenerg.* **2007**, *1767*, 1073–1101.
[25] J. Warnan, J. Willkomm, J. N. Ng, R. Godin, S. Prantl, J. R. Durrant, E. Reisner, *Chem. Sci.* **2017**, *8*, 3070–3079.
[26] J. Willkomm, K. L. Orchard, A. Reynal, E. Pastor, J. R. Durrant, E. Reisner, *Chem. Soc. Rev.* **2016**, *45*, 9–23.
[27] T. W. Woolerton, S. Sheard, E. Pierce, S. W. Ragsdale, F. A. Armstrong, *Energy Environ. Sci.* **2011**, *4*, 2393.
[28] J.-S. Lee, D.-I. Won, W.-J. Jung, H.-J. Son, C. Pac, S. O. Kang, *Angew. Chemie Int. Ed.* **2017**, *56*, 976–980.
[29] M. A. Gross, A. Reynal, J. R. Durrant, E. Reisner, *J. Am. Chem. Soc.* **2014**, *136*, 356–366.
[30] C. Wombwell, C. A. Caputo, E. Reisner, *Acc. Chem. Res.* **2015**, *48*, 2858–2865.
[31] T. W. Woolerton, S. Sheard, E. Reisner, E. Pierce, S. W. Ragsdale, F. A. Armstrong, *J. Am. Chem. Soc.* **2010**, *132*, 2132–2133.
[32] S. H. Lee, D. S. Choi, S. K. Kuk, C. B. Park, *Angew. Chemie Int. Ed.* **2018**, *57*, 7958–7985.

Table of Contents

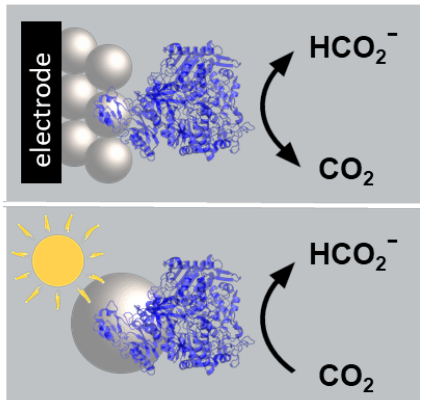

Electro- and solar-driven CO_2 utilization: Reversible electrocatalysis with formate dehydrogenase on porous metal oxides is established. A self-assembled colloidal system containing formate dehydrogenase immobilized on dye-sensitized TiO_2 provides a benchmark for selective reduction of CO_2 to formate in aqueous solution.